JOURNAL OF AIRCRAFT
Vol. 43, No. 1, January–February 2006

Wind-Tunnel Boundary Corrections for a Full-Scale 1903 Wright Flyer Replica

Wael A. Mokhtar* and Colin P. Britcher†
Old Dominion University, Norfolk, Virginia 23529-0247

A panel code is developed in order to assess and correct wind-tunnel boundary interferences during a test of a full-scale reproduction of the 1903 Wright "Flyer" in the Langley Full-Scale Tunnel (LFST). The LFST is a very large, low-speed wind tunnel with a $\frac{3}{4}$-open test section. The principal concerns relating to boundary corrections are the relatively large size of the replica relative to the test-section dimensions, coupled with the lack of modern correction techniques for aeronautical testing in open-jet test sections. The Flyer is represented either by simple lifting surfaces, with the accuracy of the representation validated by direct calculations using the panel code CMARC, or by an array of simple horseshoe vortex singularities. Vortex ring panels are used in the boundary correction code. The solution starts by solving the flow in a closed test section in order to obtain the flow properties on the boundaries. An iterative method, based on the one-step method employed in adaptive wall wind-tunnel work, is then used to adapt the boundary geometry to a constant-pressure condition. Finally the boundary interference is obtained by calculating the velocities induced in the test region by the boundary singularities. Results are presented for different test-section boundary configurations: fully closed, fully open, and $\frac{3}{4}$ open. Corrections are compared to calculations using the classical method of images.

I. Introduction

IN commemoration of the Centennial of Flight, a faithful reproduction of the Wright Brothers' "Flyer" was flown at the site of the original triumph, on 17 December 2003. The reproduction, created by the Wright Experience under the direction of Ken Hyde, is likely the most accurate yet attempted. As part of the extensive preparations for the commemorative flights, the airframe was subjected to a wind-tunnel test program in the Langley Full-Scale Tunnel (LFST), operated by Old Dominion University, as described by Britcher et al.[1] and Kochersberger et al.[2]

A previous full-scale replica had also been wind tunnel tested, as reported by Cherne et al.[3] In this test, the wing span was approximately 50% of the test-section width, and the wind-tunnel boundaries were solid walls, so that classical boundary correction techniques could be applied with some confidence. In the case of the LFST, the relatively larger wing span, just over 67% of the test-section width, coupled with the unusual $\frac{3}{4}$-open configuration, gives rise to some concerns about the accuracy and applicability of classical correction schemes. Because of the narrow performance margins and inherent instability of the Flyer, the most accurate wind-tunnel data set possible was required for development of flight simulators.[2,4] Therefore the focus of this paper is the development of a modern boundary interference correction scheme for application to the Wright Flyer reproduction (shown in Fig. 1) and to other unusually large test articles.

II. Boundary-Interference Assessment Techniques

Boundary interferences of open-jet test sections were first studied by Theodorsen[5] in the early 1930s. He used the method of images to obtain the boundary interference for several test-section configurations ranging from closed to open, including one, two, and three solid boundaries. Experimental verification of his techniques included tests in the LFST, then referred to as the NACA Full-Scale Tunnel. More recently, as reported by Cooper,[6,7] the majority of the work in boundary interference for open test sections has been undertaken for automotive wind tunnels because many large open-jet wind tunnels have been designed specifically for the development of automobiles. There remain only a few low-speed, open-jet wind tunnels still used for aeronautical testing, with the LFST as one example. Figure 2 shows a representation of the nozzle, test section, and collector of the LFST. Because the main concern in automotive testing is to correct the drag coefficient of high-blockage models, the methods used in open-jet automotive tunnels are not suitable here, because in aeronautical applications all measured forces and moments need to be corrected, not just drag, and blockage is typically small.

Contemporary methods used for boundary corrections in closed-wall test sections include the two-variable methods[8,9] and the single-variable methods.[9–11] Both rely on measurements of the flow properties on the wind-tunnel walls. These methods cannot be applied to open test sections because of experimental difficulties in detecting the boundaries of the jet and in measuring the flow properties on these boundaries.

One of the more recent methods used for wall interference correction in closed test sections is the panel method using a surface distribution of singularities on the test-section boundaries. Joppa[12] used the vortex-lattice method for the closed test section. Holt and Hunt[13] reported the use of the panel methods to correct the boundary interference of a delta wing in a rectangular test section, also the support interference. Mokry et al.[14] used the doublet-panel method for a half-model in a rectangular test section. In automotive wind tunnels, Mokry[15] used a low-order panel method for the wall interference correction to drag. Steinbach[16] used the panel method in representing the entire tunnel including the convergent part, the test section, the divergent part, an aircraft model, and its sting support system. Qian[17] validated the results obtained by a modified version of the panel code PMARC and the two-variable method for closed-wall test sections.

The panel method is considered a promising approach compared to the alternatives because it is simple, efficient, relatively fast (opening the possibility of online corrections), and it can be used with a wide range of model or test-section geometries. Ulbrich and Boone[18] used the panel method with a wall signature method for real-time wall interference correction in the Ames 12-foot pressure wind

Presented as Paper 2004-2309 at the AIAA 24th Aerodynamic Measurement Technology and Ground Testing Conference, Portland Oregon, 28 June–1 July 2004; received 13 July 2004; revision received 4 March 2005; accepted for publication 9 June 2005.

*Ph.D. Candidate/Graduate Research Assistant, Department of Aerospace Engineering. Student Member AIAA.

†Professor, Department of Aerospace Engineering. Associate Fellow AIAA.

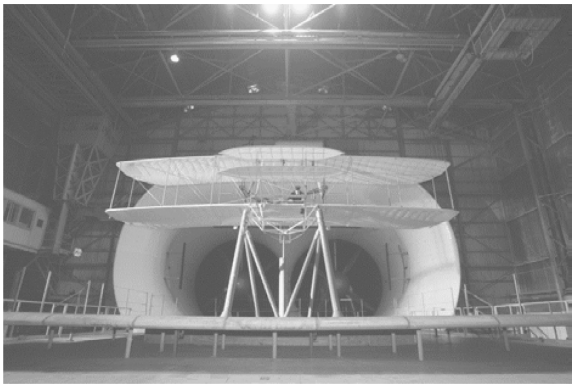

Fig. 1 Full-scale reproduction of the 1903 Wright Flyer inside the test section of the LFST.

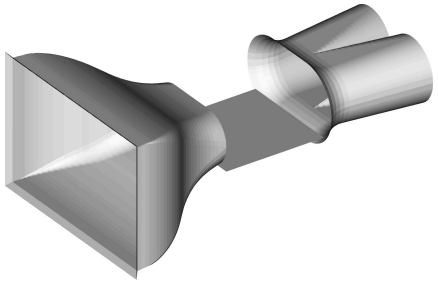

Fig. 2 Nozzle, test section, and collector of the LFST.

tunnel. Hackett[19] compared the use of the panel method and two other methods for low-speed, closed-wall tunnels and showed that the panel method is reliable.

To the best of the authors' knowledge, the vast majority of the work in boundary interference corrections using panel methods has been for closed test-section wind tunnels. The authors previously developed a low-order panel method for open test-section wind tunnels and studied the boundary interference for simple two- and three-dimensional nonlifting model representations.[20] In the present work the real geometry of the reproduction 1903 Wright Flyer is used, represented by vortex ring panels or by an assembly of simple horseshoe vortex singularities. The classical method of images is used for limited validation of the results. Derived corrections include angle of attack (upwash), canard angle to trim, blockage, and induced twist.

III. Present Method

A reference test condition is established, roughly corresponding to the predicted cruise conditions for the actual Flyer.[1] The nominal angle of attack measured to the reference axis of the landing skids is 1.5 deg, and the nominal lift coefficient is 0.58. A typical airframe drag coefficient is of the order of 0.1, with a substantial upload on the canard required to trim. The reference wing area is 510 ft^2, with the nominal wind-tunnel cross section 1607 ft^2, reduced to 1507 ft^2 when the ground board is introduced.

A. Solution Using Flyer Geometry

The first step in the present work is the development of a representation of the Flyer. Six lifting surfaces, subdivided into 720 panels, are used, as shown in Fig. 3. To ensure the accuracy of the model representation, the panel code CMARC is used to solve the flow around the entire model, and results are compared to experimental data. Figure 4 shows the results obtained by CMARC, compared to uncorrected experimental data. Fair agreement is achieved, keeping in mind that CMARC solves for solid (impermeable) surfaces while the real airframe is covered with unsealed fabric, which deforms with the airflow and allows small air leakage. The model representation is therefore considered adequate to be used, with appropriate care, in boundary-interference calculations.

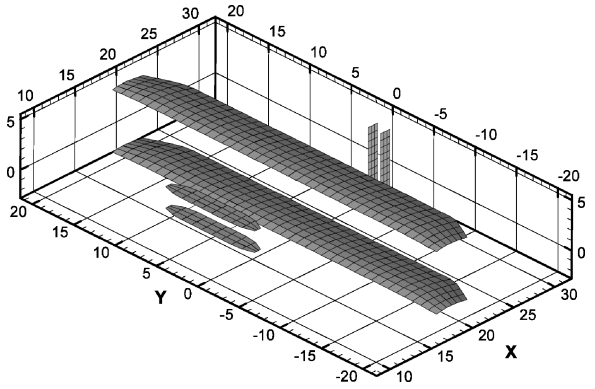

Fig. 3 Surface panels of the Wright Flyer representation.

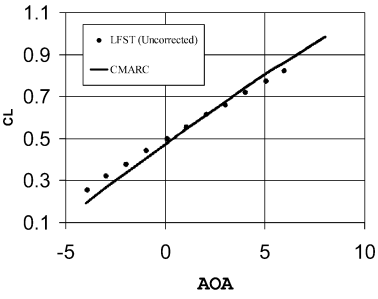

Fig. 4 Comparison between uncorrected LFST and CMARC results.

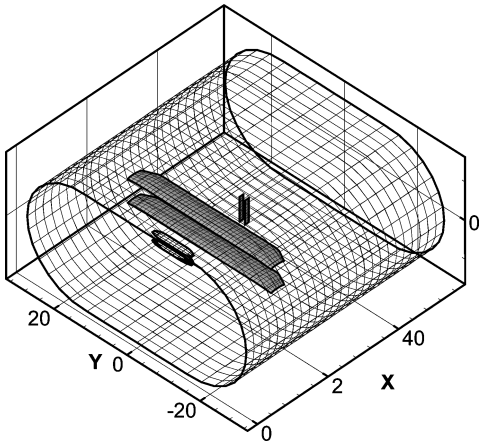

Fig. 5 Surface panel representation of the Flyer inside the test section of the LFST.

The boundary corrections are derived in two main stages. In the first stage, the test-section boundaries and the model representation are paneled, as shown in Fig. 5, with the boundary panels' strengths solved for as solid walls with zero normal velocity.

In the second stage, the boundaries are solved again with the correct open test-section boundary condition applied. An iteration method (based on the so-called "one-step" method used in adaptive wall wind-tunnel work) is used to adapt the boundary geometry to the required constant-pressure condition, using the velocity components on the boundaries obtained from the previous stage. The one-step method is described by Goodyer,[21] Wolf and Goodyer,[22] and Wedemeyer et al.[23] More details about the iteration method can be found in Mokhtar and Britcher.[20] After each boundary adaptation iteration, the domain is solved in the same way as before and the panel geometry adjusted. Finally the interference factors are obtained using the velocity components induced by the boundary panels, as shown in Eqs. (1) and (2) (Ref. 24):

$$\varepsilon = \boldsymbol{u}_i / \boldsymbol{U}_\infty \tag{1}$$

$$\Delta\alpha = \boldsymbol{w}_i / \boldsymbol{U}_\infty \tag{2}$$

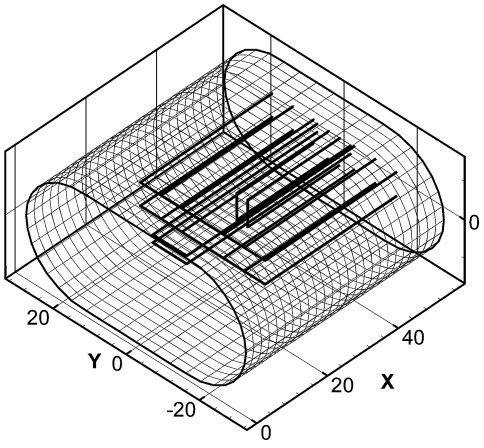

Fig. 6 Flyer representation by horseshoe vortex singularities inside the LFST.

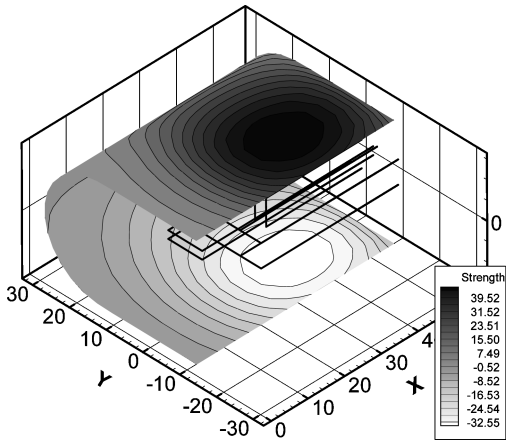

Fig. 7 Boundary singularity strengths using the horseshoe vortex representation.

where ε is the blockage interference factor, $\Delta\alpha$ is the induced angle of attack, u_i and w_i are streamwise and vertical velocity components induced by the boundary panels, and U_∞ is the freestream velocity.

The test-section representation is of finite length (equal to the actual length), leading to some sensitivity to inflow and outflow conditions. In the current work, both the inflow and outflow cross sections are fixed, with a constant axial velocity imposed far upstream and downstream. This is not a completely faithful representation of the conditions in the wind tunnel, where nozzle-exit nonuniformity can be present and where the collector entry conditions are quite complex, but is considered adequate for the current purpose.

B. Solution Using Simplified Representation

To explore the possibility of using a simple representation of the test article, also to facilitate comparison to classical image methods, the Flyer is also represented by horseshoe vortex singularities as shown in Fig. 6. The spanwise distribution and relative strengths are chosen based on a classical lifting-line solution. The solution technique is similar to the previous case except that measured forces are used to obtain the initial strengths of the horseshoe singularities for the Flyer representation. Then the boundaries are solved to obtain the corrections as before.

C. Solution Using Method of Images

Because the bulk of previously published work relating to aeronautical tests in open-jet test sections relies on the method of images, additional solutions are obtained using finite arrays of images surrounding a rectangular test section in order to add confidence to the new method and to explore the applicability of these traditional methods.

IV. Results—Interference Assessments

The effect of two parameters on the interference is considered in the present work, namely, the test-section boundary configuration (closed, open, and $\frac{3}{4}$ open) and the choice of the Flyer representation (surface panels or horseshoe vortices). Because the Flyer consists of thin lifting surfaces, with a very low blockage ratio, upwash interference is the primary focus of this comparison study.

To investigate the effect of the Flyer representation on the interference assessment, the steps of the solution are studied one by one. Figures 7 and 8 show the "signature" of the Flyer over the test-section boundaries represented by the strengths of the surface panels at the end of the first step of the solution, solving for closed boundaries, with the model represented by horseshoe vortices and by surface panels, respectively. The signatures produced by both methods exhibit the same overall characteristics with slight differences caused by the large wing span compared to test-section width, resulting in decreased accuracy of the horseshoe vortex representation. Although the differences are relatively small, they have a significant effect on the following steps of the solution, as will be shown later. Figures 9–12 show the geometry of the test section at the end of the second step, boundary deformation, for both open and $\frac{3}{4}$-open boundary configurations with the two different Flyer representations. Because the boundary deformation process depends on the flow properties on the boundaries, some differences can be seen between the boundary geometries obtained using the surface panel representation of the Flyer and the one obtained using the array of horseshoe vortices.

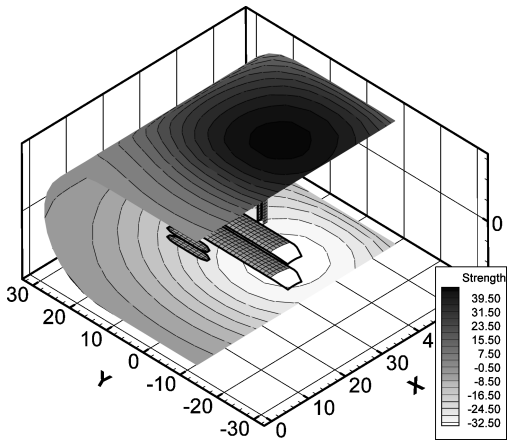

Fig. 8 Boundary singularity strengths using the surface panel representation.

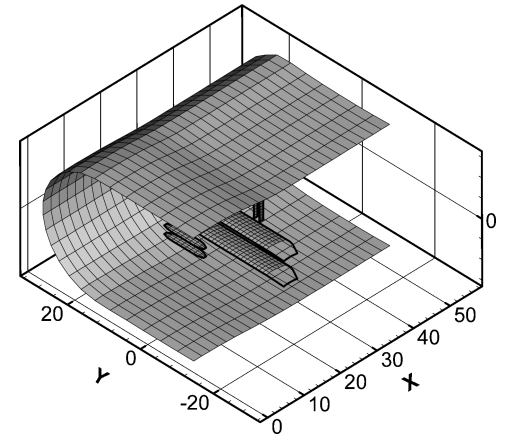

Fig. 9 Jet distortion, fully open test section; surface panel representation.

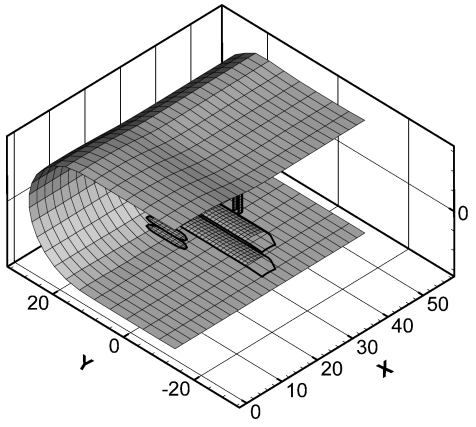

Fig. 10 Jet distortion, $\frac{3}{4}$-open test section; surface panel representation.

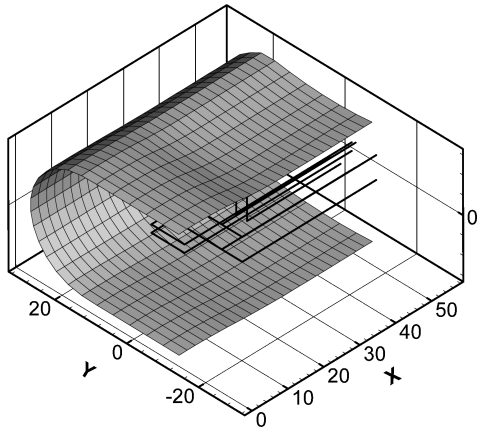

Fig. 11 Jet distortion, fully open test section; horseshoe vortex representation.

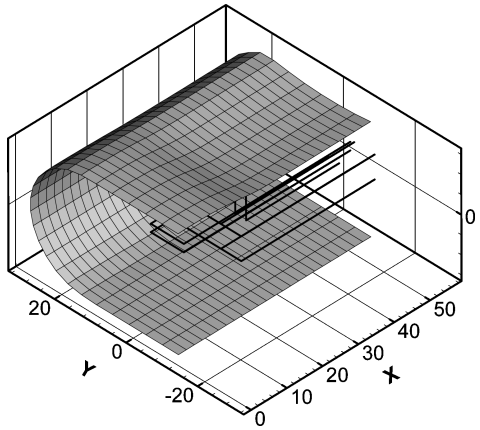

Fig. 12 Jet distortion, $\frac{3}{4}$-open test section; horseshoe vortex representation.

To investigate the effect of the test-section boundary configuration on the interference assessment, the upwash distribution is found on horizontal and vertical planes passing through the test-section centerline, for closed, open, and $\frac{3}{4}$-open test sections, using the same Flyer representation (surface panels), as shown in Figs. 13–15. The magnitude of induced upwash in the case of the closed test section is slightly less than that seen in the open test section, with opposite sign. It is also found that in the case of the $\frac{3}{4}$-open test section the interference of the solid ground board acts in the opposite sense to the rest of the boundaries, which greatly decreases the magnitude of the net induced upwash as shown in Fig. 15. For all of the test-section boundary configurations, the maximum upwash is downstream to the centroid of the wings. Relatively little effect of the boundary configuration can be seen on the distributions of upwash in the downstream or spanwise directions.

For further study of the effect of the Flyer representation on the interference assessment, similar results are obtained using the horseshoe vortex representation, as shown in Figs. 16–19. The closed test section seems to be least sensitive to the approach used for Flyer representation while in the open test section the solution is relatively more sensitive. The $\frac{3}{4}$-open test section is the most sensitive to the Flyer representation, at least in relative terms, because is has the lowest magnitude of upwash interference.

The theoretical downstream asymptote of induced upwash in a long test-section is twice the value at the location of the test article. This condition is not seen here because of the downstream constraint of the test-section cross section. Calculations with increased test-section lengths more closely match the theoretical asymptote.

From the previous study it is clear that existence of a ground plane in the $\frac{3}{4}$-open test section significantly decreases the magnitude of the boundary interference but makes the solution relatively more sensitive to the Flyer representation. In addition, the downstream gradients of the upwash are rather low for the $\frac{3}{4}$-open test section, which makes it amenable to an approach where the test conditions are corrected based on the magnitude of interference at certain points (wing or canard quarter-chords for example). This is not necessarily the case for fully closed or fully open test sections, where the downstream gradient of the upwash is relatively high and additional care would have to be taken to include the residual variance of the interferences.

To complete the interference assessment of the Flyer test, the blockage distribution on horizontal and vertical planes passing through the test-section centerline is presented in Fig. 19. Because the Flyer has a very low frontal area, the blockage corrections are one order of magnitude lower than the upwash interference, with negligible spanwise and low downstream gradients.

Classical image methods can be applied to validate the results from the high-fidelity calculations just discussed. The upwash factor δ can be estimated for the case of rectangular test sections, from classical charts,[25] or by numerical calculations with a large array of images. Here, the horseshoe vortex representation just described is used for a numerical calculation of a 101×101 array of images, assuming an infinite test-section length. Calculated upwash angles at the midwing centerline quarter-chord for a 30×60 ft rectangular test section are shown in Table 1. Table 2 summarizes the geometry

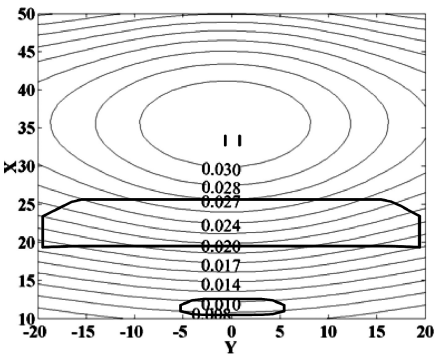

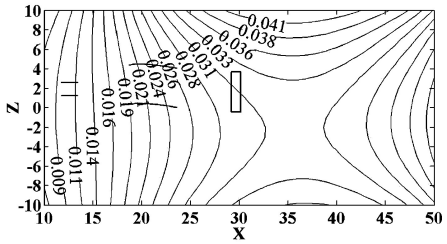

Fig. 13 Upwash interference for closed test section; surface panel representation.

Table 1 Upwash angles for the reference case ($C_L = 0.58$), various test sections, method of images

Test-section configuration	Small wing span, deg	Actual Flyer span
Closed rectangular, 30 × 60 ft	1.3	1.05 deg (root); 0.65 deg (tip)
Open rectangular, 30 × 60 ft	−2.5	−2.1 deg (root); −1.4 deg (tip)
$\frac{3}{4}$-open rectangular, 30 × 60 ft	−0.2	−0.2 deg (root); −0.4 deg (tip)
Closed rectangular 30 × 54 ft	1.4	1.1 deg (root); 0.9 deg (tip)
Open rectangular 30 × 54 ft	−2.5	−2.1 deg (root); −1.5 (tip)
$\frac{3}{4}$-open rectangular 30 × 54 ft	−0.3	−0.3 deg (root); −0.6 deg (tip)

Table 2 Summary of geometry of wing representation by horseshoe vortices

Component	Spanwise coordinates, ft	Height above tunnel C/L, ft	Relative strength
Lower wing	17.13 to −17.0	−1.36	1.0
	11.42 to −11.33	−1.36	0.432
	5.71 to −5.66	−1.36	0.103
Upper wing	17.13 to −17.0	4.82	1
	11.42 to −11.33	4.82	0.432
	5.71 to −5.66	4.82	0.103

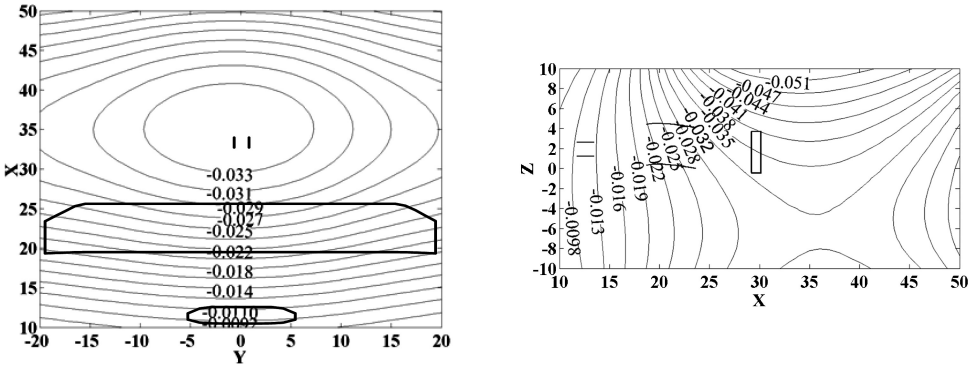

Fig. 14 Upwash interference for open test section; surface panel representation.

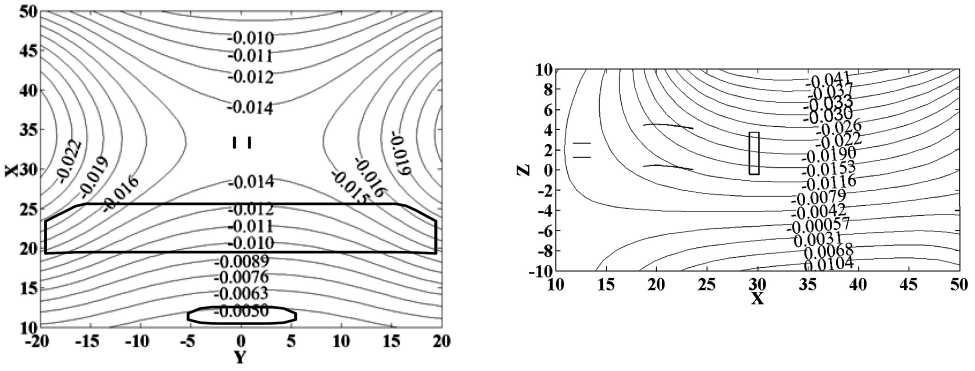

Fig. 15 Upwash interference for $\frac{3}{4}$-open test section; surface panel representation.

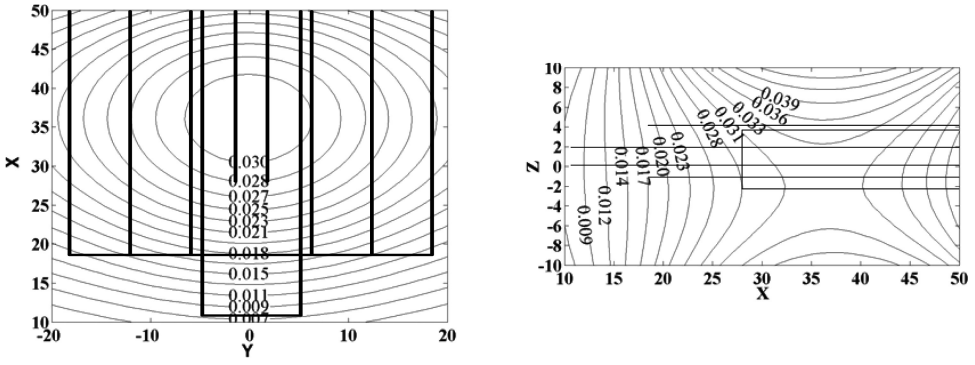

Fig. 16 Upwash interference for closed test section; horseshoe vortex representation.

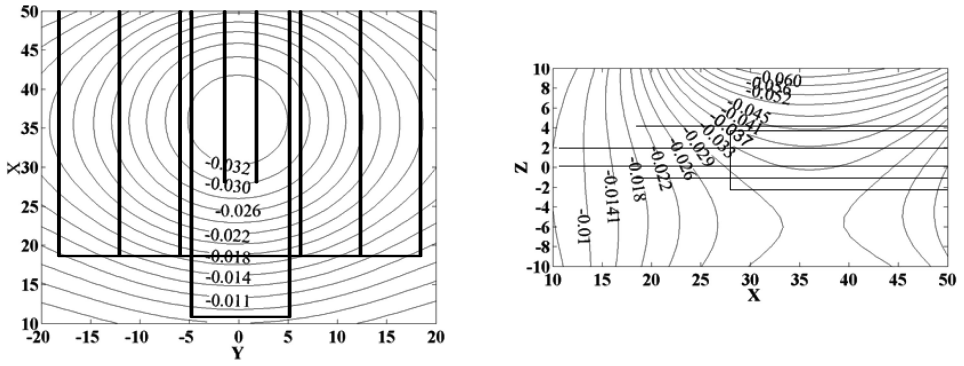

Fig. 17 Upwash interference for open-jet test section: horseshoe vortex representation.

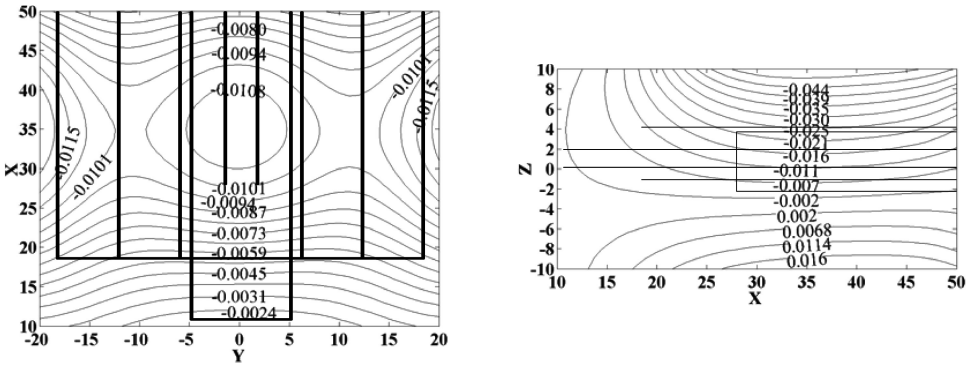

Fig. 18 Upwash interference for $\frac{3}{4}$-open test section; horseshoe vortex representation.

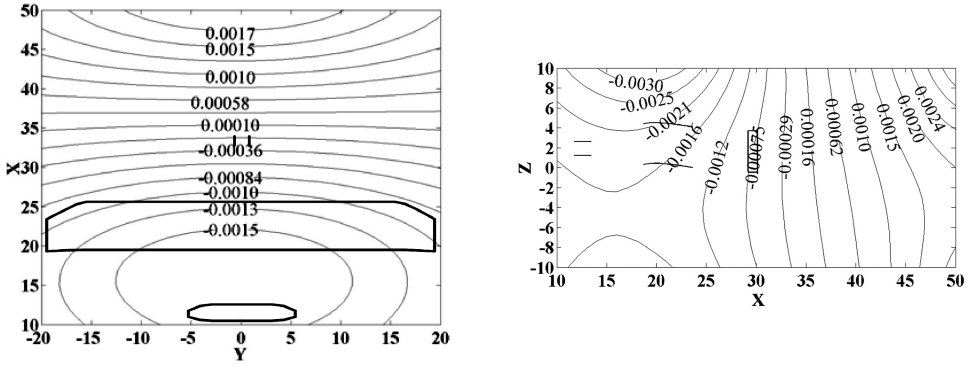

Fig. 19 Blockage interference for $\frac{3}{4}$-open test section; surface panel representation.

of the horseshoe vortex array. The vortex strengths are adjusted to give the same lift as the reference case. The Flyer is slightly asymmetric, with the starboard wings 4 in. longer than the port wings.

This test-section geometry clearly underestimates the effects of the lateral boundaries, and so calculations are repeated for a modified test section with the width adjusted to give more or less the same total flow area as the actual tunnel. An image array for the actual test-section cross section, which nominally comprises two 30-ft diameter semicircles bounding a 30×30 ft square, cannot easily be established. The orders of magnitude of the upwash angles estimated by image methods are seen to be broadly consistent with the calculations just described, as summarized in Figs. 16–18.

V. Results—Application of Corrections

Full treatment of the magnitude of the corrections and their effects on the aerodynamic data acquired during the wind-tunnel tests of the Flyer is beyond the scope of this paper. However, some statements concerning the order of magnitude can be made, based on the reference case just described, followed by correction of a representative angle-of-attack sweep. The Flyer's wing quarter-chord line was located at around the 21-ft station in x, with the aircraft wings nearly equidistant above and below the y axis. Figure 15 indicates that the average induced upwash across the wing quarter-chord locations is around -0.0105 or -0.60 deg. Because the measured lift curve slope $C_{L\alpha}$ is approximately 0.054 per degree, this suggests a lift coefficient correction of only 0.032, which is around 5% of the nominal value. The corresponding drag coefficient correction would be only 0.006, again only a few percent of the nominal value. Figure 20 shows the effect of applying the corrections for induced upwash on a representative lift curve, following well-established procedures.[25] The upper and lower wings are exposed to different levels of upwash, and a spanwise upwash gradient exits, with maximum values on centerline, falling to near zero at the tips. For reference, the induced twist

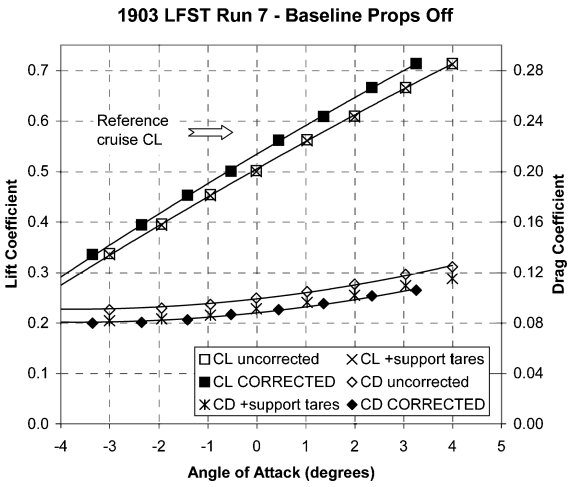

Fig. 20 Corrected lift curve.

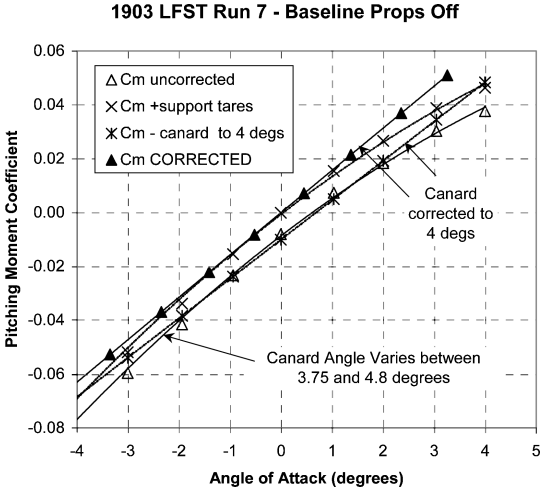

Fig. 21 Corrected pitching-moment curve.

is around 0.3 deg, averaged over the two wings. The effects of the induced twist are typically not considered correctable.

The streamwise gradient in upwash is rather small. Figure 15 shows an induced upwash at the canard location of perhaps -0.005, or -0.29 deg, leading to small corrections of canard angle to trim because this is less than the average value at the wing. Figure 21 shows the effect of the canard angle corrections. It is seen that the magnitudes of the structural deflections of the canard under load are larger than the boundary-induced corrections. These deflections arise as a result of the canard being pivoted about the 50% chord location, resulting in increased "nose-up" deflection as aerodynamic loads increase. Blockage effects on aerodynamic results are completely negligible.

VI. Conclusions

A panel code to assess and correct wind-tunnel boundary interferences during a test of a full-scale 1903 Wright Flyer replica in the LFST was successfully developed. Induced upwash and upwash gradients in the LFST's large test section were the main concerns. Blockage was very low and does not have a significant effect on the aerodynamic test results. A comparison study between different test-section boundary configurations (closed, open, and $\frac{3}{4}$ open) showed that the existence of the ground board in the $\frac{3}{4}$-open test-section geometry decreases the interference by an order of magnitude compared to either a closed or fully open test section. Also, comparing different approaches to representing the Flyer (surface panels or horseshoe vortices) it was found that the closed test section is least sensitive, whereas the $\frac{3}{4}$-open test section is the most sensitive in relative terms. The magnitudes of corrections to angle of attack, lift and drag coefficients, canard angle to trim, and induced wing twist are all surprisingly small, considering the relatively large size of the Flyer reproduction relative to the test-section dimensions. Corrections can thus be applied to the Flyer data set with high confidence.

Acknowledgments

The Wright Flyer reproduction was made available by the Wright Experience, under the leadership of Ken Hyde. Wind-tunnel time was provided by the Langley Full-Scale Tunnel, an Enterprise Center of the Batten College of Engineering and Technology at Old Dominion University. The analysis and interpretation of the wind-tunnel results has been a team effort, with input from Kevin Kochersberger of Rochester Institute of Technology, Jack Ralston and Jenn Player of Birhle Applied Research, Norm Crabill of Vigyan Incorporated, and many others.

References

[1]Britcher, C., Landman, D., Ash, R., and Hyde, K., "Predicted Flight Performance of the Wright 'Flyer' Based on Full-Scale Tunnel Data," AIAA Paper 2004-104, Jan. 2004.

[2]Kochersberger, K., Britcher, C., Crabill, N., Player, J., and Hyde, K., "Flying Qualities of the Wright 1903 Flyer: From Simulation to Flight Test," AIAA Paper 2004-105, Jan. 2004.

[3]Cherne, J., Culick, F., and Zell, P., "The AIAA 1903 Wright 'Flyer' Project Prior to Full-Scale Tests at NASA Ames Research Center," AIAA Paper 2000-0511, Jan. 2000.

[4]Ralston, J., Kochersberger, K., Britcher, C., and Hyde, K., "1903 Wright Flyer Simulator for Flight Support and Training," AIAA Paper 2004-4825, Aug. 2004.

[5]Theodoresen, T., "The Theory of Wind Tunnel Wall Interference," NACA Rept. No. 410, Oct. 1931, pp. 219–227.

[6]SAE International, "Aerodynamic Testing of Road Vehicles in Open-Jet Wind Tunnels," Society of Automotive Engineers, SP-1465, May 1999.

[7]Cooper, K., 'Bluff-Body Blockage Correction in Closed and Open Test Section Wind Tunnels," AGARD, AG-336, NTIS, Springfield, VA, 1998, pp. 6.1–6.33.

[8]Ashill, P. R., "Boundary-Flow Measurement Methods for Wall Interference Assessment and Correction—Classifications and Review," AGARD, CP-535, 1994, pp 12.1–12.21.

[9]Ashill, P. R., Hackett, J. E., Mokry, M., and Steinle, F., "Boundary-Flow Measurement Methods," AGARD, AG-336, NTIS, Springfield, VA, 1998, pp. 4.1–4.61.

[10]Hackett, J. E., "Tunnel-Induced Gradients and their Effect on Drag," *AIAA Journal*, Vol. 34, No. 12, 1996, pp. 2575–2581.

[11]Hackett, J. E., and Wilsden, D. J., "Determination of Low Speed Blockage Corrections via Tunnel Wall Static Pressure Measurements," AGARD, CP-174, NTIS, Springfield, VA, 1976, pp. 22.1–22.9.

[12]Joppa, R. G., "A Method of Calculating Wind Tunnel Interference Factor for Tunnels of Arbitrary Cross Section," NASA CR-845, July 1967.

[13]Holt, D. R., and Hunt, B., "The Use of Panel Methods for the Evaluation of Subsonic Wall Interference," AGARD, CP-335, NTIS, Springfield, VA, 1982, pp. 2.1–2.16.

[14]Mokry, M., Digney, J. R., and Poole, R. J. D., "Double-Panel Method for Half-Model Wind Tunnel Corrections," *Journal of Aircraft*, Vol. 24, No. 5, 1987, pp. 322–327.

[15]Mokry, M., "Wall Interference Correction to Drag Measurements in Automotive Wind Tunnels," *Journal of Wind Engineering and Industrial Aerodynamics*, Vol. 56, May 1995, pp. 107–122.

[16]Steinbach, D., "Calculation of Wall and Model Support Interference in Subsonic Wind Tunnel Flows," *Zeitschrift für Flugwissenschaften und Weltraumforschung*, Vol. 17, No. 36, 1993, pp. 370–378.

[17]Qian, X., "A Study of Wind Tunnel Aerodynamic Data Correction with Panel Methods and the Two-Variable Method," Ph.D. Dissertation, Dept. of Mechanical Engineering, Univ. of Tennessee, Knoxville, Dec. 1994.

[18]Ulbrich, N., and Boone, A., "Real-Time Wall Interference Correction System of the 12 ft Pressure Wind Tunnel," AIAA Paper 98-0707, Jan. 1998.

[19]Hackett, J., "Recent Developments in the Calculation of Low-Speed Solid-Walled Tunnel Wall Interference in Tests on Large Models, Part I:

Evaluation of Three Interference Assessment Methods," *Progress in Aerospace Science*, Vol. 39, Aug. 2003, pp. 537–583.

[20]Mokhtar, W., and Britcher, C., "Boundary Interference Assessment and Correction for Open Test Section Wind Tunnels Using Panel Methods," AIAA Paper 2004-609, Jan. 2004.

[21]Goodyer, M. J., "A Low Speed Self-Streamlining Wind Tunnel," AGARD, CP-174, Dept. of Mechanical Engineering, 1976, pp. 13.1–13.8.

[22]Wolf, S. W. D., and Goodyer, M. J., "Predictive Wall Adjustment Strategy for Two-Dimensional Flexible Walled Adaptive Wind Tunnel—A Detailed Description of the First One-Step Method," NASA CR-181635, Jan. 1988.

[23]Wedemeyer, E., Taylor, N. J., and Holst, H., "Adaptive Wall Techniques," AGARD, AG-336, Dept. of Mechanical Engineering, 1998, pp. 10.1–10.48.

[24]Krynytzky, A., and Ewald, B., "Conventional Wall Correction for Closed and Open Test Sections," AGARD, AG-336, Dept. of Mechanical Engineering, 1998, pp. 2.1–2.66.

[25]Barlow, J. B., Rae, W. H., and Pope, A., *Low Speed Wind Tunnel Testing*, 3rd ed., Wiley, Hoboken, NJ, 1999, Chaps. 8–10.